Theoretical study of shallow acceptor states under the influence of both a confinement potential and a deformation potential

Q. X. Zhao and M. Willander
Physical Electronics and Photonics, Department of Microelectronics and Nanoscience, Chalmers University of Technology and Göteborg University, S-412 96 Göteborg, Sweden
(Received 27 August 1997; revised manuscript received 22 December 1997)

Energy levels of the ground and the excited shallow acceptor states have been calculated for center-doped strain-free GaAs/$Al_xGa_{1-x}As$ quantum wells (QW's) in the presence of an external pressure and in strained $In_xGa_{1-x}As/Al_yGa_{1-y}As$ QW's. The impurity states are calculated using a four-band effective-mass theory, in which the valence-band mixing as well as the mismatch of the band parameters and the dielectric constants between well and barrier materials have been taken into account. The acceptor binding energies and the internal electronic transitions are calculated. The results show that an applied external pressure in GaAs/$Al_xGa_{1-x}As$ QW's or built-in strain in $In_xGa_{1-x}As/Al_yGa_{1-y}As$ QW's strongly influences the acceptor states. The oscillator strengths between the acceptor ground states and the different excited p-like states are also calculated for the $In_xGa_{1-x}As/Al_{0.3}Ga_{0.7}As$ system with three different indium fractions x. The results show clearly that a built-in strain strongly influences the transition energies and the relative oscillator strengths. [S0163-1829(98)05720-8]

I. INTRODUCTION

A comprehensive understanding of the acceptors confined in lattice matched quantum well (QW) structures during the last decay, has been achieved through extensive experimental[1–10] and theoretical[11–17] investigations. Corresponding study of impurities confined in strained systems, such as $In_xGa_{1-x}As$ and nitride-based structures (both with great application potential), is very limited. The purpose of this theoretical study is to gain a more detailed understanding of the acceptor electronic structures under the influence of both the QW confinement and the deformation potential.

Because of the complexity of such calculations, the number of reports in the literature that deal with the presence of a deformation potential is very limited. Schmidt[18] has analytically discussed the splitting of acceptor ground states and their shift under the influence of axial stress or noncubic crystal field on the basis of a spherical or cubic valence-band structure with large spin-orbit splitting in bulk material. Recently the N acceptors confined in strained $Cd_xZn_{1-x}Te$ QW structures were reported experimentally.[19] To the best of our knowledge, the only theoretical and experimental work that takes into consideration the strain dependence of the acceptors in QW structures was reported by Loehr *et al.*[20] However, the excited states of acceptors have so far, to our knowledge, not been studied.

In this theoretical investigation, we employ a well-established theoretical model to calculate the ground states and the excited states of acceptors that are subjected to an influence from both a confinement potential and a deformation potential. Our calculation is based on the method that was previously used for calculating acceptor levels in strain-free GaAs/$Al_xGa_{1-x}As$ QW structures with and without an external magnetic field as a perturbation[12,13,15–17] We demonstrate the influence of compressive and tensional strains on the binding energies of the different acceptor states, the energy splitting of the acceptor ground states, and the transition energies between the $1S$ and the $2S$ states. The paper is organized in the following way: In Sec. II, we briefly discuss how the strain effects are included in the theory. In Sec. III, we present the results from strained $In_xGa_{1-x}As/Al_yGa_{1-y}As$ QW's and results from strain-free GaAs/$Al_xGa_{1-x}As$ QW's in the presence of an applied external pressure.

II. BRIEF DESCRIPTION OF THE THEORY

The effective-mass theory applied in this study is based on earlier work.[12,13] It has been successfully applied in strain-free systems with and without an applied external magnetic field as a perturbation.[12,13,15–17] To calculate strained systems, we need to properly include the strain effects in the acceptor Hamiltonian. In the following we briefly discuss the strain effects in the theoretical model. Consider a single QW grown in the [001] direction (which we take as the quantization axis z), the acceptor Hamiltonian expressed in electron energy is given by a 4×4 matrix operator,[12]

$$H=-[H^{\mathrm{kin}}+H^{c}+H_{p}^{\mathrm{qw}}]. \tag{1}$$

Here H^{kin} represents the kinetic energy of the hole, H_p^{qw} contains the confinement potential due to the valence-band discontinuity and the influence of a deformation potential, and H^c is the potential of the acceptor impurity center and of the image charges due to the mismatch of the dielectric constant. The details of H^{kin} and H^c can be found in Ref. 12.

The modification of the QW potential, H_p^{qw} must include the effects of the deformation potential. That is, H_p^{qw} will contain a square-well potential, $H_{\mathrm{hh,lh}}^{\mathrm{qw}}$, for the heavy hole (hh) and the light hole (lh), and includes a potential difference (V_p) between the hh and lh band edges in the well (due to built-in or external strain);

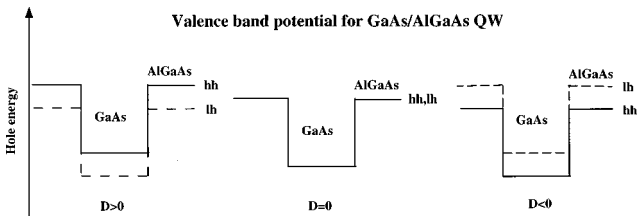

FIG. 1. A schematic drawing of valence band potential of a GaAs/Al_xGa_{1-x}As QW structure under different sign of the biaxial deformation potential.

$$H_p^{\mathrm{qw}} = H_{\mathrm{hh,lh}}^{\mathrm{qw}} + V_p \,. \tag{2}$$

Note that unlike previous reports,[11–17] here $H_{\mathrm{hh,lh}}^{\mathrm{qw}}$ may have different values for the hh and lh states when the deformation potential is included. In the case of strain-free QW's (i.e., the barrier materials and the well material have a similar stress coefficient) an applied external stress only changes the energy separation (V_p) between the hh and lh state and $H_{\mathrm{hh,lh}}^{\mathrm{qw}}$ will not change. The splitting between the hh and lh states due to an applied pressure can be described by $V_p(\pm 3/2) = -V_p(\pm 1/2) = D$ in Eq. (2). If D is zero, we have the exact situation that was reported earlier.[12,13,15–17] In our definition, a negative D means that the stress potential has a compressive character. In that case, the hh state will be the ground state. On the other hand, when D is positive we have a tensional strain situation, and the lh state will be the ground state. Figure 1 shows the case of Al_xGa_{1-x}As/GaAs QW's under different external strain conditions. If the barrier and well layers have different stress coefficients, the stress dependence of $H_{\mathrm{hh,lh}}^{\mathrm{qw}}$ must also be treated properly. In the case of lattice mismatched QW systems, it is clear that the built-in strain influences both the hh and lh band offset $H_{\mathrm{hh,lh}}^{\mathrm{qw}}$ and the energy separation V_p in Eq. (2).

Once the strain effects are properly included in the acceptor Hamiltonian, the Hamiltonian given in Eq. (1) acts on this four-component function F^m,

$$HF^m = EF^m. \tag{3}$$

The energy levels of the shallow acceptor states and corresponding wave functions are derived. $F^m(r,q,z) = [F^{m,s}] = [F^{m,3/2}, F^{m,1/2}, F^{m,-1/2}, F^{m,-3/2}]$, and the s component of an acceptor envelope function of definite angular momentum m can be expanded into a set of basis functions, separable in the coordinates ρ and z;

$$F^{m,s}(\rho,\theta,z) = e^{i(m-s)\theta} f^{m,s}(\rho,z) = e^{i(m-s)\theta} \sum_n R_n^{m,s}(\rho) g_n^s(z). \tag{4}$$

The function g_n^s is chosen to be the s component of the four-component envelope function g_n, which describes a QW subband state at $\mathbf{k}_\parallel = 0$. The potential difference between the hh and lh in Eq. (2), further complicates the computer program.

III. RESULTS AND DISCUSSIONS

We first examine the strain-free GaAs/Al_xGa_{1-x}As system in the presence of an external stress. This gives an idea of how the deformation potential influences the acceptor binding energies without changing the band offset potential (which determines the confinement effect). In the following numerical calculations, the Luttinger parameters[21] given in Table I are used. The parameters for the Al_xGa_{1-x}As alloy are obtained by a linear interpolation between the GaAs and the AlAs parameters. An offset ratio between the conduction and the valence band of 65–35 has been assumed and the valence-band discontinuity for the Al_xGa_{1-x}As alloy is accordingly taken as $\Delta E_v = 0.35 \times 1.247x$ eV. Since the $Al_{0.3}Ga_{0.7}$As alloy and GaAs has similar stress coefficients, an applied stress will not change the valence-band offset. It will only change the energy separation between the hh and lh states by $V_p(\pm 3/2) = -V_p(\pm 1/2) = D$ [Eq. (2)].

TABLE I. The Luttinger parameters. The parameters of alloy, linear interpolation of two binary material parameters, except for the band-gap energy of alloy In_xGa_{1-x}As and spin-orbit splitting of alloy In_xGa_{1-x}As. They are given by $E_g(In_xGa_{1-x}As) = E_g(GaAs) - 1.5837x + 0.475x^2$ (eV) and $\Delta_{so}(In_xGa_{1-x}As) = \Delta_{so}(GaAs) - 0.09x + 0.14x^2$ (eV).

	GaAs	InAs	AlAs
γ_1	6.85	20.40	3.45
γ_2	2.10	8.30	0.68
γ_3	2.90	9.10	1.29
ε	12.53	15.15	9.80
a (Å)	5.653 25	6.0583	5.653 25
Δ_{so}	0.34	0.38	
C_{12}/C_{11}	0.5071	0.5434	
a_v (eV)	1.16	1.0	
b (eV)	−2.0	−1.8	

The pressure dependence of the lowest-energy levels for the center-doped acceptors in 100-Å-wide GaAs/$Al_{0.3}Ga_{0.7}$As QW is calculated. Figure 2 shows the even symmetric acceptor states. Solid and dashed curves cor-

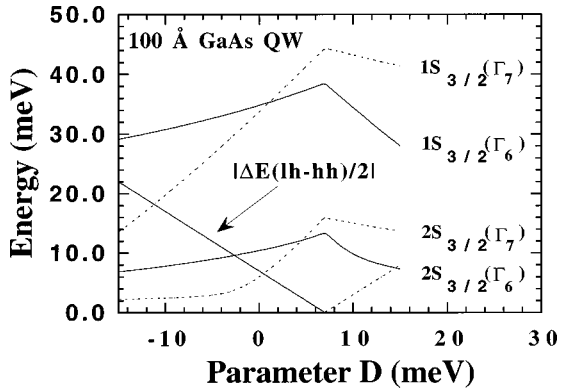

FIG. 2. Pressure dependence of the binding energy of the even parity acceptor states for an on-center impurity in a 100-Å-wide GaAs/$Al_{0.3}Ga_{0.7}$As QW. Solid and dashed curves are used for states of the $(3/2,+)$ and $(1/2,+)$ symmetry, respectively. The binding energies are given with respect to the bottom of the first hole subband. The energy separation $|\Delta E(\text{lh-hh})|$ between the first lh and the first hh sublevel is also indicated in the figure. The solid line for $|\Delta E(\text{lh-hh})|$ corresponding to that of the ground state is the hh state and the dashed line for $|\Delta E(\text{lh-hh})|$ corresponding to that of the ground state is the lh state.

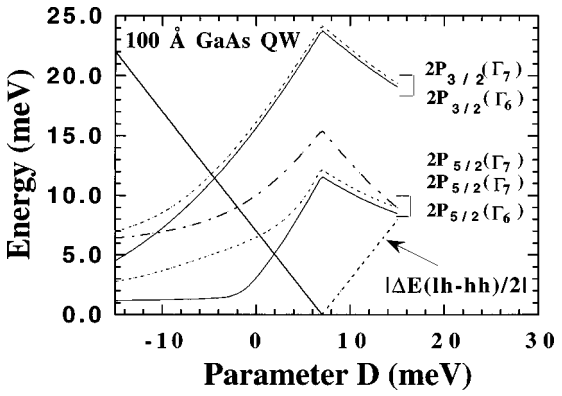

FIG. 3. Pressure dependence of the binding energy of the odd parity acceptor states for an on-center impurity in a 100-Å-wide $GaAs/Al_{0.3}Ga_{0.7}As$ QW. Solid, dashed, and dotted-dashed curves are used for states of the $(1/2,-)$, $(3/2,-)$, and $(5/2,-)$ symmetry, respectively. The binding energies are given with respect to the bottom of the first hole subband. The energy separation $|\Delta E(\text{lh-hh})|$ between the first lh and the first hh sublevel is also indicated in the figure. The solid line for $|\Delta E(\text{lh-hh})|$ corresponding to that of the ground state is the hh state and the dashed line for $|\Delta E(\text{lh-hh})|$ corresponding to that of the ground state is the lh state.

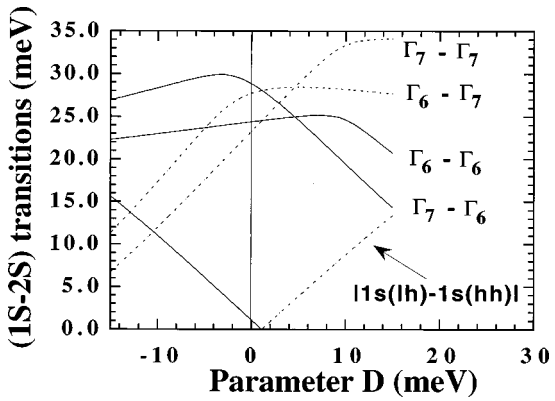

FIG. 4. Pressure dependence of transitions from the $1S$ acceptor states to the excited S-like acceptor states in a 100-Å-wide $GaAs/Al_{0.3}Ga_{0.7}As$ QW. The energy separation $|1S(\text{lh})\text{-}1S(\text{hh})|$ between the ground $1S$ lh-like acceptor and the ground $1S$ hh-like acceptor state is also indicated in the figure. The solid line of $|1S(\text{lh})\text{-}1S(\text{hh})|$ corresponding to that of the ground state has the heavy-hole character and the dashed line of $|1S(\text{lh})\text{-}1S(\text{hh})|$ corresponding to that of the ground state has the light-hole character.

respond to states with $(3/2,+)$ and $(1/2,+)$ symmetry, respectively. The fourfold degenerate acceptor ground state in bulk, $1S_{3/2}(\Gamma_8)$, splits into two twofold degenerate states, $1S_{3/2}(\Gamma_6)$ and $1S_{3/2}(\Gamma_7)$, for acceptors located at the center of the QW. The $1S_{3/2}(\Gamma_6)$ and $1S_{3/2}(\Gamma_7)$ states are related to the hh ground state of $(3/2,+)$ symmetry and the lh ground state of $(1/2,+)$ symmetry, respectively. The acceptor energies are given with respect to the bottom of the first hole subband, which corresponds to the energy of the lowest hole level in an impurity-free QW. Worthy of note is the fact that (depending on the strength and the sign of the deformation potential and the QW confinement) the ground state can be either the hh or lh state. In the case of a 100-Å $GaAs/Al_{0.3}Ga_{0.7}As$ QW, the crossover between the first hh and the first lh sublevels occurs at a value of $D=7.0$ meV. It is also of interest to note that in Fig. 2 the crossover between the ground acceptor states, $1S_{3/2}(\Gamma_6)$ and $1S_{3/2}(\Gamma_7)$, occurs before the crossover of the first hh and lh subbands. If we assume a very simple proportional relation between the acceptor ground splitting and the first heavy-light hole subband splitting, the results in Fig. 2 suggest that the deformation potential has a stronger influence than the confinement potential, on the acceptor ground-state splitting relative to the first hh-lh subband splitting. Otherwise, there are two possibilities: (1) we would expect the crossover between the ground acceptor states to occur after the crossover of the first hh and lh subbands or (2) the acceptor ground states degenerate when the first hh-lh subbands degenerate. The actual occurrence depends on whether the deformation potential has a weaker or a similar influence on the acceptor ground-state splitting relative to the first hh-lh subband splitting in comparison with the confinement potential.

Figure 3 shows the binding energies of the odd symmetric acceptor states. Solid, dashed, and dotted-dashed curves illustrate the pressure dependence of states with $(1/2,-)$, $(3/2,-)$, and $(5/2,-)$ symmetry, respectively. In a QW, the bulk states $2P_{3/2}$ and $2P_{5/2}$ split into doublet states.

In infrared absorption measurements, the transitions between the $1S$ ground state and the different excited S-like states are forbidden. However, the $1S$-$2S$ energy separation can be deduced from selective photoluminescence and resonant Raman measurements.[6,10,15] Figure 4 shows the energy separations between the ground state $[1S_{3/2}(\Gamma_6)$ and $1S_{3/2}(\Gamma_7)]$ and the excited states $[2S_{3/2}(\Gamma_6)$ and $2S_{3/2}(\Gamma_7)]$. On the other hand, the transitions from the $1S$ ground state to different odd symmetric excited states (P-like states) are dipole allowed transitions in infrared absorption measurements, such as the transitions denoted G, D, and C lines in bulk GaAs material corresponding to the transitions from the $1S_{3/2}(\Gamma_6)$ and the $1S_{3/2}(\Gamma_7)$ ground states to the $2P_{3/2}$ and the $2P_{5/2}$ excited states. The transition energy can be deduced from Figs. 2 and 3. The results are not shown here since they are difficult to measure. The difficulty lies in the weak absorption through the thin doping layer, particularly under external pressures. The $1S$-$2S$ transitions are more conveniently measured by selective photoluminescence via two-hole transitions or its Raman components in QW structures. Due to thermalization effects, the $1S$-$2S$ transitions related to the hh acceptor ground state $[1S_{3/2}(\Gamma_6)]$ will dominate when the D value is negative. The $1S$-$2S$ transitions related to the lh acceptor ground state $[1S_{3/2}(\Gamma_7)]$ will dominate when D has a positive value.

For strained QW systems, a built-in strain changes both the hh and lh band offset as well as the energy separation between them. Here we consider the $In_xGa_{1-x}As/Al_yGa_{1-y}As$ system. As previously mentioned, the parameters for GaAs and AlAs are given in Table I. For $In_xGa_{1-x}As/GaAs$ an offset ratio between the conduction and the valence bands of 60–40 has been used.[22] The difference of the band-gap energy between strain-free $In_xGa_{1-x}As$ alloy and GaAs is accordingly taken as $\Delta E=(1.5837x-0.475x^2)$ eV.[23] The biaxial deformation is given by $\varepsilon=[a_0-a(x)]/a(x)$. The shear stress energy for the hh and lh states is $\zeta_{\text{hh}}=-\varepsilon_0=b[1+(2C_{12}/C_{11})]\varepsilon$, $\zeta_{\text{lh}}=-(\Delta_{\text{so}}-\varepsilon_0)/2+(\Delta_{\text{so}}/2)\sqrt{[1+(2\varepsilon_0/\Delta_{\text{so}})+9(\varepsilon_0/\Delta_{\text{so}})^2]}$, respectively.[24,25] Δ_{so} is a parameter of spin-orbit splitting. It is

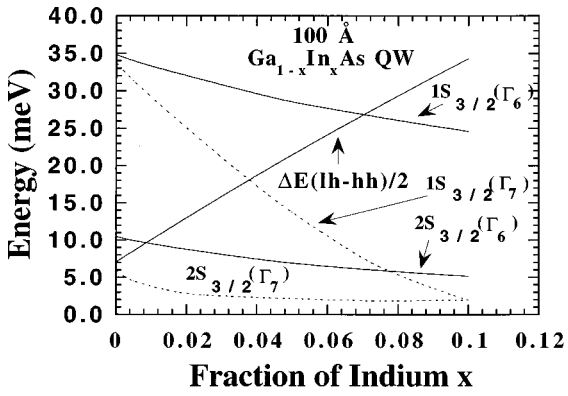

FIG. 5. The binding energy of the even parity acceptor states for an on-center impurity in a 100-Å-wide $In_xGa_{1-x}As/Al_{0.3}Ga_{0.7}As$ QW vs different fractions x of indium. Solid and dashed curves are used for states of the $(3/2,+)$ and $(1/2,+)$ symmetry, respectively. The binding energies are given with respect to the bottom of the first heavy-hole subband. The energy separation $|\Delta E(\text{lh-hh})|$ between the first lh and the first hh sublevels is also indicated in the figure.

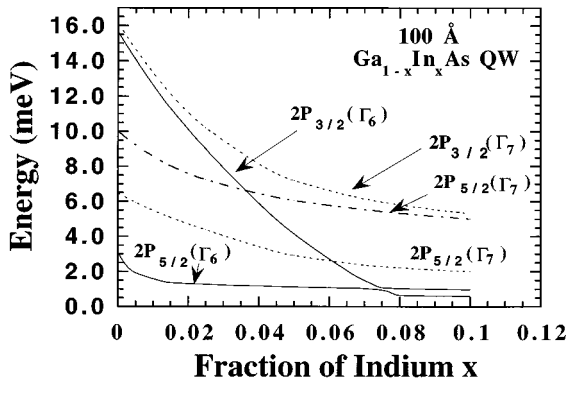

FIG. 6. The binding energy of the odd parity acceptor states for an on-center impurity in a 100-Å-wide $In_xGa_{1-x}As/Al_{0.3}Ga_{0.7}As$ QW vs different fractions x of indium. Solid, dashed, and dotted-dashed curves are used for states of the $(1/2,-)$, $(3/2,-)$, and $(5/2,-)$ symmetry, respectively. The binding energies are given with respect to the bottom of the first heavy-hole subband.

given by $\Delta_{so}(x)=[\Delta_{so}(\text{GaAs})-0.09x+0.14x^2)$ eV.[23] The change of valence-band offset due to the hydrostatic stress energy is given by $2a_v[1-(C_{12}/C_{11})]\varepsilon$. Parameter a_0 is the lattice constant of the substrate, and $a(x)$ is the lattice constant of the corresponding well layer. Quantities b and a are the deformation potential constants, and C_{12} and C_{11} are the stiffness constants. The valence-band offset is given by

$$\Delta E_{\text{hh}}(\text{In}_x\text{Ga}_{1-x}\text{As/GaAs})=\left[0.4\times(1.5837x-0.475x^2)+2a_v\left(1-\frac{C_{12}}{C_{11}}\right)\varepsilon+\zeta_{\text{hh}}\right]\ \text{eV}, \tag{5}$$

$$\Delta E_{\text{lh}}(\text{In}_x\text{Ga}_{1-x}\text{As/GaAs})=\left[0.4\times(1.5837x-0.475x^2)+2a_v\left(1-\frac{C_{12}}{C_{11}}\right)\varepsilon+\zeta_{\text{lh}}\right]\ \text{eV}. \tag{6}$$

With two exceptions, the parameters for the $In_xGa_{1-x}As$ alloy are obtained by a linear interpolation between the InAs and the GaAs parameters. The exceptions are the band-gap energy and the parameter of spin-orbit splitting. These parameters are given by a quadratic relation.[23] The valence-band offset for $In_xGa_{1-x}As/Al_yGa_{1-y}As$ can thus be deduced from a relation $\Delta E_v(x,y)=\Delta E_v(\text{In}_x\text{Ga}_{1-x}\text{As/GaAs})+\Delta E_v(\text{GaAs/Al}_y\text{Ga}_{1-y}\text{As})$. Due to a built-in strain, the band offsets of the hh and lh states are different now. The energy separation between the hh and lh bands is given by $V_p=-(\zeta_{\text{hh}}-\zeta_{\text{lh}})$. The parameters used for the calculations are listed in Table I. It is important to point out that the band offset ratio in the range of 70/30 to 60/40 in the $In_xGa_{1-x}As/GaAs$ system has been reported,[22,23] and the value is referred to the strained band-gap energy. Thus by using Eqs. (5) and (6), we have overestimated the strain contribution in the band offset. However, we use the $In_xGa_{1-x}As/Al_{0.3}Ga_{0.7}As$ system; therefore, the maximum overestimate presented in this study is 6% of the total valence-band offset. This causes a negligible influence on the calculated acceptor binding energies and oscillator strengths shown in Figs. 5–9.

Figures 5–7 show the corresponding S-like states, P-like states, and $1S$-$2S$ transition energies of acceptors confined in the center of $In_xGa_{1-x}As/Al_{0.3}Ga_{0.7}As$ QW's for different indium fractions. Since the lattice constant of $In_xGa_{1-x}As$ is larger than the lattice constant of $Al_xGa_{1-x}As$, the $In_xGa_{1-x}As/Al_yGa_{1-y}As$ QW structures have a built-in compressive strain. The results should show a trend similar to that for $GaAs/Al_xGa_{1-x}As$ under compressive pressure (which is in fact consistent with Fig. 5, if compared with Fig. 2 for the case of $D<0$). The dramatic changes of acceptor binding energy versus concentration of indium are demonstrated in Figs. 5 and 6. Particularly evident there is the split-

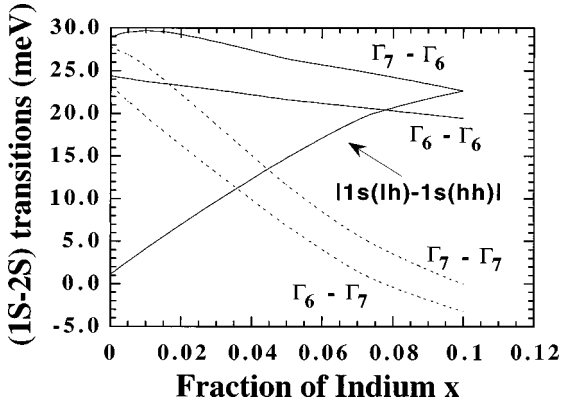

FIG. 7. The transitions from the $1S$ hole acceptor states to the excited S-like acceptor states in a 100-Å-wide $In_xGa_{1-x}As/Al_{0.3}Ga_{0.7}As$ QW vs different indium fractions x. The energy separation $|1S(\text{lh})\text{-}1S(\text{hh})|$ between the ground $1S_{3/2}(\Gamma_7)$ acceptor state and the ground $1S_{3/2}(\Gamma_6)$ acceptor state is also indicated in the figure.

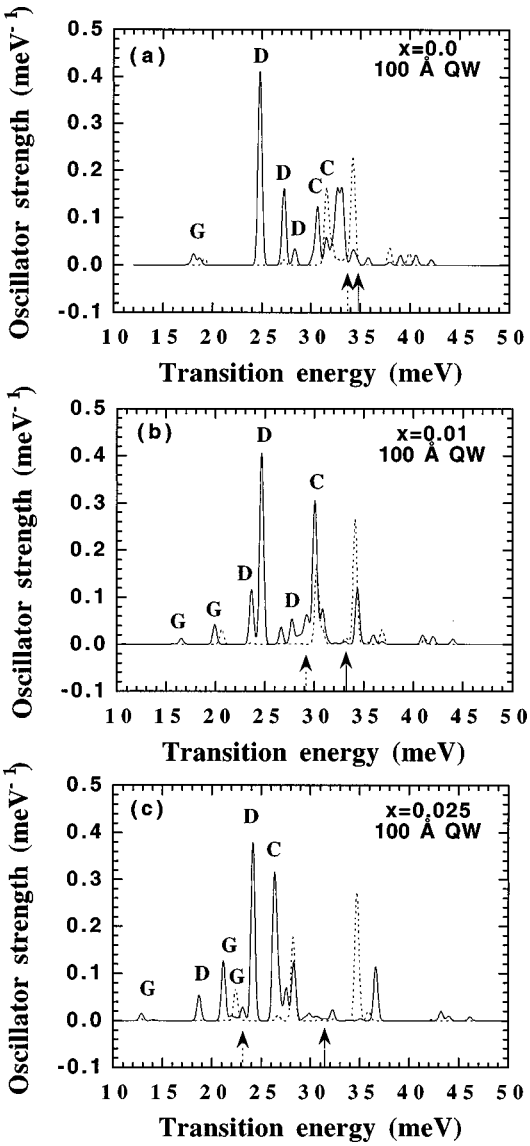

FIG. 8. The oscillator strengths of the absorption lines from the $1S_{3/2}(\Gamma_6)$ and $1S_{3/2}(\Gamma_7)$ acceptor states vs the transition energy for x (solid lines) and z (dashed lines) polarization in $In_xGa_{1-x}As/Al_{0.3}Ga_{0.7}As$ QW's with (a) $x=0.0$, (b) $x=0.01$, and (c) $x=0.025$. The thermal population effect is not included in the figure.

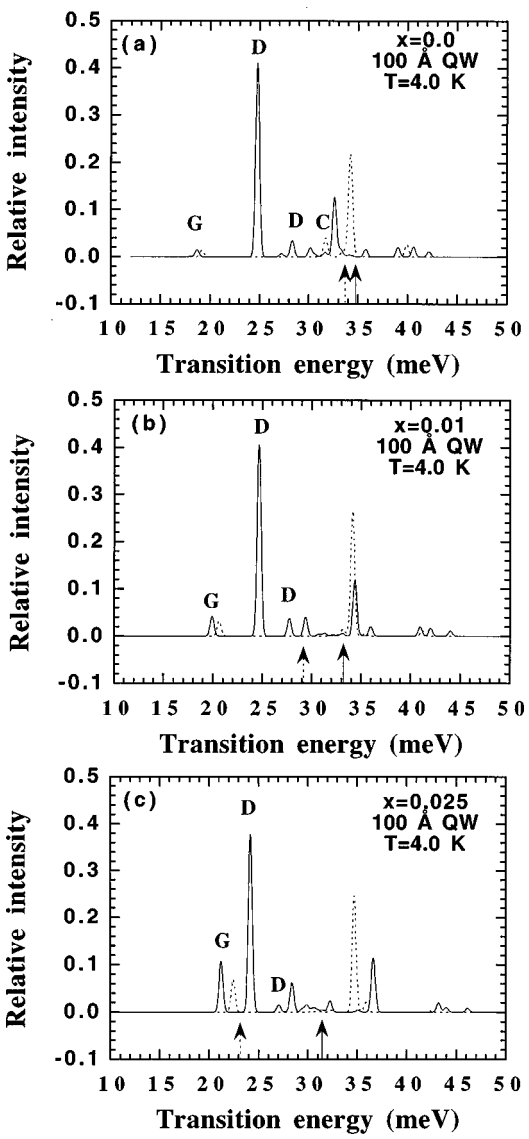

FIG. 9. The relative strengths of the absorption lines at 4.0 K from the $1S_{3/2}(\Gamma_6)$ and $1S_{3/2}(\Gamma_6)$ acceptor states vs the transition energy for x (solid lines) and z (dashed lines) polarization in $In_xGa_{1-x}As/Al_{0.3}Ga_{0.7}As$ QW's with (a) $x=0.0$, (b) $x=0.01$, and (c) $x=0.025$.

ting of the ground acceptor states $[1S_{3/2}(\Gamma_6)$ and $1S_{3/2}(\Gamma_7)]$. The results indicate that most likely only the $1S$-$2S$ transitions related to the hh ground acceptor state $1S_{3/2}(\Gamma_6)$ can be observed experimentally in selective photoluminescence measurements when the indium fraction is more than 0.02 due to large energy separation between the $1S_{3/2}(\Gamma_6)$ and $1S_{3/2}(\Gamma_7)$ states.

The oscillator strengths between the acceptor ground states and the different excited p-like states[13,17] are also calculated for the $In_xGa_{1-x}As/Al_{0.3}Ga_{0.7}As$ system with three different indium fractions x, according to the following formula:[13]

$$f_{i0}(\varepsilon)=\frac{2m_0(E_i-E_0)}{2\hbar^2\gamma_1}\sum_{k,k'}\sum_{s}|\langle F^s_{ik'}|\boldsymbol{\varepsilon}\cdot\mathbf{r}|F^s_{0k}\rangle|^2, \quad (7)$$

where f_{i0} is the oscillator strength of transitions from the ground state to the excited state labeled by i. E_0, F^s_{0k} and E_i, $F^s_{ik'}$ are the energies and envelope functions of ground and excited states, respectively, and $\boldsymbol{\varepsilon}$ is the polarization vector of the electromagnetic radiation. The results are shown in Figs. 8 and 9. A Gaussian broadening is introduced for all transitions with a Gaussian broadening parameter of 0.2 meV. The solid (dashed) arrow indicates the transition energy between the acceptor $1S_{3/2}(\Gamma_6)$ and $1S_{3/2}(\Gamma_7)$ ground states and the continuum, respectively. The energy separation between the two arrows corresponds to the energy splitting of the acceptor ground states. The solid and dashed lines in the figures correspond to the x- and z-polarization transitions.[13,17] In Fig. 8, the effect of the thermal population in the acceptor ground states $1S_{3/2}(\Gamma_6)$ and $1S_{3/2}(\Gamma_7)$ is not included. The data represent an oscillator strength of each transition only. The transitions corresponding to the bulk no-

tations G, D, and C are also identified in the figures. They show clearly that a built-in strain strongly influences the transition energies and the relative oscillator strengths. The relative intensity of the transitions from the $1S_{3/2}(\Gamma_6)$ and $1S_{3/2}(\Gamma_7)$ ground states depends not only on the oscillator strengths but also on the relative population of the two ground states. In order to compare the calculated results with experimental data, we have to consider the relative occupation of the $1S_{3/2}(\Gamma_6)$ and $1S_{3/2}(\Gamma_7)$ ground states. Occupation of these states is determined by the Boltzman factor, i.e., $n(\Gamma_7)/n(\Gamma_6)=\exp(-\Delta_{\text{hh-lh}}/kT)$. Here $\Delta_{\text{hh-lh}}$ represents the energy splitting between the $1S_{3/2}(\Gamma_7)$ and $1S_{3/2}(\Gamma_6)$ acceptor ground states. In Fig. 9, the relative intensity of the transitions from the ground states is demonstrated at $T=4.0$ K. The transitions related to the $1S_{3/2}(\Gamma_7)$ ground state are hardly seen at this temperature.

In summary, a well-developed four-band effective-mass model has been used to calculate the acceptor states in strain-free QW's in the presence of an applied pressure and in a system with a built-in strain. The transitions between the $1S$ acceptor state and the excited S-like states are deduced. The results show that the biaxial deformation potential can strongly influence the acceptor binding energy and the splitting of the ground $1S$-like acceptor state. Our calculated results are ready to be compared with the $1S$-$2S$ energy separations determined by selective PL measurements via the THT satellites. The oscillator strengths between the acceptor ground states and the different excited p-like states are also calculated for the $In_xGa_{1-x}As/Al_{0.3}Ga_{0.7}As$ system with three different indium fractions x. The results show clearly, that a built-in strain strongly influences the transition energies and the relative oscillator strengths.

ACKNOWLEDGMENTS

The authors would like to thank P. O. Holtz for many valuable discussions and comments, and A. Pasquarello for many discussions concerning the previous theoretical calculations for acceptors confined in a QW system and for providing computer codes for the modifications.

[1] R. C. Miller, A. C. Gossard, W. T. Tsang, and O. Munteanu, Phys. Rev. B **25**, 3871 (1982).
[2] X. Liu, A. Petrou, B. D. McCombe, J. Ralston, and G. Wicks, Phys. Rev. B **38**, 8522 (1988).
[3] P. O. Holtz, M. Sundaram, R. Simes, J. L. Merz, A. C. Gossard, and J. H. English, Phys. Rev. B **39**, 13 293 (1989).
[4] P. O. Holtz, M. Sundaram, K. Doughty, J. L. Merz, and A. C. Gossard, Phys. Rev. B **40**, 12 338 (1989).
[5] P. O. Holtz, Q. X. Zhao, B. Monemar, M. Sundaram, J. L. Merz, and A. C. Gossard, Phys. Rev. B **47**, 15 675 (1993).
[6] P. O. Holtz, Q. X. Zhao, A. C. Ferreira, B. Monemar, M. Sundaram, J. L. Merz, and A. C. Gossard, Phys. Rev. B **48**, 8872 (1993).
[7] A. A. Reeder, B. D. McCombe, F. A. Chambers, and G. P. Devane, Phys. Rev. B **38**, 4318 (1988).
[8] B. V. Shanabrook, J. Comas, T. A. Perry, and R. Merlin, Phys. Rev. B **29**, 7096 (1984).
[9] D. Gammon, R. Merlin, W. T. Masselink, and H. Morkoc, Phys. Rev. B **33**, 2919 (1986).
[10] Q. X. Zhao, P. O. Holtz, C. I. Harris, B. Monemar, and E. Veje, Phys. Rev. B **50**, 2023 (1994).
[11] W. T. Masselink, Y.-C. Change, and H. Morkoc, Phys. Rev. B **28**, 7373 (1983); **32**, 5190 (1985).
[12] A. Pasquarello, L. C. Andreani, and R. Buczko, Phys. Rev. B **40**, 5602 (1989).
[13] S. Fraizzoli and A. Pasquarello, Phys. Rev. B **42**, 5349 (1990); **44**, 1118 (1991).
[14] G. T. Einevoll and Y.-C. Chang, Phys. Rev. B **41**, 1447 (1990).
[15] Q. X. Zhao, P. O. Holtz, A. Pasquarello, B. Monemar, A. C. Ferreira, M. Sundaram, J. L. Merz, and A. C. Gossard, Phys. Rev. B **49**, 10 794 (1994).
[16] Q. X. Zhao, P. O. Holtz, A. Pasquarello, B. Monemar, and M. Willander, Phys. Rev. B **50**, 2393 (1994).
[17] Q. X. Zhao, A. Pasquarello, P. O. Holtz, B. Monemar, and M. Willander, Phys. Rev. B **50**, 10 953 (1994).
[18] M. Schmidt, Phys. Status Solidi B **79**, 533 (1977).
[19] Q. X. Zhao, T. Baron, K. Saminadayar, and N. Magnea, J. Appl. Phys. **79**, 2070 (1995).
[20] J. P. Loehr, Y. C. Chen, D. Biswas, P. K. Bhattacharya, and J. Singh, *Proceeding of the 20th International Conference on the Physics of Semiconductors* (World Scientific, Singapore, 1990), Vol. 2, p. 1404.
[21] J. M. Luttinger, Phys. Rev. **102**, 1030 (1956).
[22] V. A. Wilkinson, A. D. Prins, D. J. Dunstan, L. K. Howard, and M. T. Emeny, J. Electron. Mater. **20**, 509 (1991).
[23] G. Arnaud, J. Allegre, P. Lefebvre, H. Mathieu, L. K. Howard, and D. J. Dunstan, Phys. Rev. B **46**, 15 290 (1992).
[24] F. H. Pollak and M. Cardona, Phys. Rev. **172**, 816 (1968).
[25] T. Lundström, J. Dalfors, P. O. Holtz, Q. X. Zhao, B. Monemar, G. Landgren, and J. Wallin, Phys. Rev. B **54**, 10 637 (1996).